Journal of Quantitative Spectroscopy & Radiative Transfer 124 (2013) 1–10

Contents lists available at SciVerse ScienceDirect

Journal of Quantitative Spectroscopy & Radiative Transfer

journal homepage: www.elsevier.com/locate/jqsrt

Line mixing in the 60-GHz atmospheric oxygen band: Comparison of the MPM and ECS model

D.S. Makarov [a,*], M.Yu. Tretyakov [a], C. Boulet [b]

[a] IAP RAS, Ulyanov str. 46, 603950 Nizhny Novgorod, Russia
[b] Université Paris-sud 11, CNRS, Institut des Sciences Moleculaires d'Orsay, Campus d'Orsay, Bat. 350, 91405 Orsay-Cedex, France

ARTICLE INFO

Article history:
Received 11 November 2012
Received in revised form
11 February 2013
Accepted 14 February 2013
Available online 27 February 2013

Keywords:
Molecular oxygen
Microwave spectroscopy
Profile shape modeling
Collisional coupling

ABSTRACT

Precise profiles of the 60-GHz molecular oxygen band recorded earlier in a wide temperature range by means of a resonator spectrometer at atmospheric pressure were treated. High signal-to-noise ratio allows careful study of the band shape taking into consideration the mixing effect. Comparative analysis of the band profile calculated by an extended MPM (Millimeter-wave Propagation Model) and by the ECS (Energy Corrected Sudden) approximation model is presented. Some limitations of the MPM approach are discussed on the basis of the comparison of the two models. Interbranch coupling is shown to make a noticeable contribution to absorption which means that it should be taken into account as it is expected to improve band profile modeling accuracy.

1. Introduction

Molecular oxygen is one of the main atmospheric absorbers of millimeter-wave radiation. Precise information on the microwave spectrum of molecular oxygen is of a great importance for various applications, such as atmosphere sensing, wireless communication, etc. Molecular oxygen has a strong band between 50 and 70 GHz and a single spectral line at 118.75 GHz. Both band and line are formed by fine structure magnetic dipole transitions within pure rotational triplets. According to the sign of the full angular momentum change, these transitions are usually denoted as $N+$ and $N-$(reference information on the mentioned transitions can be found in [1–4]). The line mixing (or collisional coupling) effect has a strong impact on the band absorption profile at atmospheric pressure, hence, it should be taken into account in radiation propagation models. Due to this influence, observed profile of the 118-GHz line does not correspond to Van Vleck-Weisskopf profile (first mentioned in [5] and experimentally studied in [6–8]), and the observed band profile does not correspond to the sum of Van Vleck-Weisskopf profiles calculated for each line forming the band either. A general approach to the shape of the bands formed by overlapping lines is given in [9,10]. A model considering the mixing effect to the first order in pressure was first proposed for the 60-GHz molecular-oxygen band in [1], and, later, a more thorough description with extension to the second order was given in [11]. Based on this approach, the Millimeter-wave Propagation Model (MPM, [3,4,12]) was developed for the aforementioned applications. The latest version of the MPM [12] provides a more detailed approach to the description of the collisional coupling effect. At the same time, it still does not provide agreement with measured absorption within experimental noise. This fact stimulates further improvement of the band profile modeling methods allowing for collisional coupling, the importance of which in applications, especially at low temperatures, was demonstrated in [13,14].

Fig. 3 of [13] shows the change in the calculated brightness temperature of the Earth's atmosphere up to 7 K under the condition of 10% change of mixing parameters (MPM

* Corresponding author. Tel.: +78314164866.
E-mail address: dmak@appl.sci-nnov.ru (D.S. Makarov).
URL: http://www.mwl.sci-nnov.ru (D.S. Makarov).

0022-4073/$ - see front matter © 2013 Elsevier Ltd. All rights reserved.
http://dx.doi.org/10.1016/j.jqsrt.2013.02.019

was used for the mentioned calculations). We should notice that 10% change is very significant and leads to the modification of the absorption band profile approximately to the same percentage of the band magnitude. The current paper is concerned with comparison of the MPM approach [12] to the 60-GHz molecular-oxygen band profile modeling with the ECS (Energy Corrected Sudden) approach. The change in the calculated absorption given by the ECS model is small, it does not exceed 1% of the band magnitude at -30 °C, so this may lead to modification of the calculated brightness temperature by the value of the order of 1 K or less. This 1% uncertainty of the calculated absorption is generally sufficient for the majority of applications, as far as it is the same order or less than various systematic measurements errors. But, at the same time, it exceeds statistical measurement uncertainties of modern atmosphere sensing instruments, and in future measurements accuracy will only increase and this will also require precise models. The ECS calculations are a little slower than the MPM ones. However, with the rapidly developing computational power it is highly probable that in the nearest future the ECS model will be used as easily as the MPM model.

The data set used for the models comparison was obtained previously in course of work [12], where details of the experiment can be found. Short experimental guidelines are given below. All the measured absorption band profiles were obtained at pressure in the 740–760 Torr range which corresponds to normal atmospheric pressure. Absorption measurements were performed by means of a BWO-based broadband resonator spectrometer equipped with a the climatic chamber allowing maintenance of stable temperature of the studied gas sample [15] and precise measurement of its temperature, pressure and humidity. Measurements were carried out in the 245–334 K temperature range. The statistical noise level of the obtained 60 GHz band profile records was about 0.01 dB/km, which permits precise analysis of the band shape using various models with allowance for collisional coupling.

2. General equations

According to [16], the absorption coefficient α at frequency value f can be expressed as

$$\alpha(f)=\frac{8\pi^3 fn}{3hc}(1-e^{-hf/k_BT})\mathrm{Im}(Tr(\rho\mathbf{dd}^{\top}[\mathbf{I}f-\mathbf{f}_0-iP\mathbf{W}]^{-1})), \quad (1)$$

where $\mathbf{I}$ is the diagonal unity matrix, k_B is the Boltzman constant, h is the Planck constant, n is the concentration of the absorbing molecules, T is the temperature, $\mathbf{d}$ is the vector of dipole momenta of the considered transitions, ρ is the diagonal matrix of the population density (ρ_{kk} defines the population of the initial level of k-th transition), $\mathbf{f}_0$ is the diagonal matrix of the transition central frequencies, P is the total pressure, and $\mathbf{W}$ is the relaxation matrix which defines all collisional effects including redistribution of the absorption intensity in the band caused by molecular collisions. The latter may be obtained by pure quantum-mechanic calculation [17] or semi-empirical methods [18]. The size of the relaxation matrix depends on the number of transitions taken into account. For microwave spectra of oxygen one should consider $N+$ and $N-$ fine structure transitions at positive and negative frequencies and, also, non-resonant transitions. Transitions at positive and negative frequencies with photon absorption occur between the same energy levels [19]. In the latter case, photon negative energy is compensated according to the energy conservation equation by thermal energy of the collisionally interacting molecules. Being sufficiently broadened by collisions, negative-frequency transitions give rise to absorption value at positive frequencies. Non-resonant transitions have zero frequency and appear because selection rules require molecular state parity conservation for magnetic-dipole transitions, which allows transitions with the same initial and final state. Three series of non-resonant transitions can be distinguished: 0^0 and $0^{\pm}$, which correspond to transitions $J=N\rightarrow J=N$ and $J=N\pm1\rightarrow J=N\pm1$, respectively.

Because of the large size of $\mathbf{W}$ due to a large number of lines that must be taken into account according to their contribution in the absorption profile, analytical matrix inversion in (1) is almost impossible, so one should use numerical inversion or use approximate methods. To invert the matrix in expression (1), the perturbation theory is appropriate under the condition

$$\left|\frac{PW_{lk}}{f_l-f_k}\right|\ll 1, \quad (2)$$

where l, k are line indexes and f_l, f_k are the corresponding central frequencies. Taking into account the first- and the second-order pressure terms, the expression for the absorption coefficient is written as [11]

$$\alpha(f)=\sum_i C_i f^2\left(\frac{\gamma_i P\cdot(1+g_iP^2)+y_iP\cdot(f-f_i-\delta\nu_iP^2)}{\gamma_i^2P^2+(f-f_i-\delta\nu_iP^2)^2}+\frac{\gamma_iP\cdot(1+g_iP^2)-y_iP\cdot(f+f_i+\delta\nu_iP^2)}{\gamma_i^2P^2+(f+f_i+\delta\nu_iP^2)^2}\right). \quad (3)$$

In the expression (3) α (e.g. in dB/km; hereinafter units used in this work are given in parenthesis) is absorption coefficient, the sum is taken over all lines in the band, i is the individual line index, C_i (dB/km GHz) is the line amplitude, P (Torr) is pressure, γ_i (GHz/Torr) is the line broadening coefficient, f_i (GHz) is the line central frequency, y_i(1/Torr) is the first-order mixing coefficient, g_i (1/Torr^2) and $\delta\nu_i$ (GHz/Torr^2) are second-order mixing coefficients accounting for mixing of line intensities and line central frequencies, respectively. The profile (3) taken with only first-order pressure terms was first proposed in [1] and later used in the MPM [3].[1] In the MPM, the influence of non-resonant absorption was modeled as a single line with $i=0$ at zero frequency with intensity equal to total intensity of non-resonant lines and broadening coefficient equal to average weighted broadening coefficients of non-resonant lines.

[1] Hereinafter, the profile (3) taken with non-zero first-order mixing parameters is referred to as the "first-order MPM profile", and the one taken with non-zero first- and second-order mixing parameters is referred to as the "second-order MPM profile".

It is worthy of notice that the broadening coefficient of the k-th line is defined by the real part of the relaxation matrix diagonal elements [20]:

$$\gamma_k = \mathrm{Re}(W_{kk}).$$

The imaginary part of W_{kk} defines the k-th line central frequency shift linearly depending on pressure. As was shown in [4], this shift is negligibly small for molecular oxygen fine-structure lines and W_{kk} can be considered to be real. First- and second-order mixing coefficients are determined through combinations of the **W** matrix non-diagonal elements (see [1] and [11] for details). The condition (2), as well as the expressions for mixing coefficients include the lines central frequencies differences in the denominator. In [1] it was mentioned that there are four line pairs violating condition (2): $1+$ and $15-$, $9-$ and $3+$, $5-$ and $7+$, $13+$ and $3-$ because of close values of central frequencies of the mentioned lines. In [1] and, descending later, in [11,21,3], this problem was solved by neglecting the parts of **W** responsible for inter-branch coupling, due to the dominating contribution of intra-branch coupling on the basis of Lam's pure quantum mechanics calculation [17]. This assumption makes **W** block-diagonal and rather simple for calculation.

3. ECS methods for W matrix

The ECS (Energy Corrected Sudden) formalism is the method for calculation of a relaxation matrix based on semi-empirical molecular collision cross-section calculation. It is based on the IOS (Infinite-Order Sudden) formalism proposed earlier by Corey and McCourt [22]. Further it was suggested for molecular oxygen A-band shape description by H. Tran et al within pure Hund's case b [18]. In contrast to the MPM relaxation matrix calculation approximations mentioned in Section 2, the ECS approach has no a priori suggestions for the pattern of coupling between various line series ($N\pm$ at positive and negative frequencies and $0^{\pm}$, 0^0 at zero frequencies) and, therefore, **W** is no longer considered as block-diagonal. Nevertheless, when applying the ECS formalism to the 60-GHz molecular oxygen band, we still use two assumptions:

- Like in the MPM calculations, working within pure Hund's case b we neglect coupling between fine-structure lines ($\Delta N = 0$) and rotational lines ($\Delta N = \pm 2$) which do not even exist in this approximation.
- We neglect rotational structure of perturber molecule. Moreover, in the absence of precise data on the pure oxygen absorption which would be able to provide information on oxygen–oxygen collisions, we consider and calculate relaxation matrix for an "air molecule" as a single object, not the proportional sum of separately obtained matrices for collisions with oxygen and nitrogen molecules taken weighed as 0.21 and 0.79, respectively.

Two properties intrinsic for the **W** matrix are detailed balance and sum rule [23]:

$$W_{lk}\rho_{kk} = W_{kl}\rho_{ll},$$

$$\sum_l d_l W_{lk} = 0, \tag{4}$$

where W_{lk} is the matrix element for coupling of the transition $k \equiv (N_k J_k) \to (N_k J_k')$ to the transition $l \equiv (N_l J_l) \to (N_l J_l')$, d_l is the reduced dipole moment of transition l:

$$d_l = (-1)^{J_l'+N}\sqrt{6(2J_l'+1)(2J_l+1)}\begin{Bmatrix} 1 & 1 & 1 \\ J_l & J_l' & N \end{Bmatrix}. \tag{5}$$

In the expression (5), $\{\ldots\}$ denotes 6-J coefficient. Sum rule is helpful to link the calculated ECS matrix to the experimentally measured broadenings W_{kk}, as far as their values are given only relative to other matrix elements (see Eq. (7) below). Since the ECS formalism deals with downwards cross-sections only, i.e. it allows calculation of matrix elements W_{lk} where rotational energy $E_{rot}(N_k J_k) > E_{rot}(N_l J_l)$, detailed balance will be used to calculate upward cross-sections for pairs of transitions where $E_{rot}(N_k J_k) < E_{rot}(N_l J_l)$. Considering coupling of the transition k to the transition l, the ECS matrix element can be written as

$$W_{lk} = \sum_L (-1)^{J_k+J_l+L+1}[N_k][N_l]\sqrt{[J_k][J_l][J_k'][J_l']}\frac{\Omega(N_k)}{\Omega(L)} \times \begin{pmatrix} N_l & N_k & L \\ 0 & 0 & 0 \end{pmatrix}\begin{Bmatrix} L & J_k & J_l \\ 1 & N_l & N_k \end{Bmatrix}\begin{Bmatrix} L & J_k' & J_l' \\ 1 & N_l & N_k \end{Bmatrix}\begin{Bmatrix} L & J_k & J_l \\ 1 & J_l' & J_k' \end{Bmatrix} Q_L, \tag{6}$$

where $[X] \equiv \sqrt{2X+1}$, $(\cdots)$ is 3-J coefficient and $\{\cdots\}$ is 6-J coefficient. Parameters Q_L are identified as basic inelastic collision cross-sections of a spinless oxygen molecule:

$$Q_L \equiv \sigma(0 \to L) = (2L+1)\sigma(L \to 0),$$

which is associated with the excitation from the $J=0$ to the $J=L$ rotational level (note that in terms of [18], the notation $Q_L = \sigma(L \to 0)$ is used). The cross-sections are commonly modeled with the exponential-polynomial dependence

$$Q_L = C_{ste}\frac{2L+1}{(L(L+1))^{\alpha}}\exp\left(-\beta\frac{E_{rot}(L)}{k_B T}\right). \tag{7}$$

To consider rotation of the molecule during the collision, adiabaticity factors $\Omega(N)$ are introduced according to [24]

$$\Omega(N) = \left(1+\tfrac{1}{24}(\omega_{N,N-2}\tau_c)^2\right)^{-2}, \tag{8}$$

where $\omega_{N,N-2} = (E_N - E_{N-2})/\hbar$, parameter $\tau_c = d_c/\overline{v}$ gives the average duration of the collision, $\overline{v}$ is average molecular relative speed and d_c is scale length (an inherent intermolecular potential specific distance).

The expression (6) has four parameters: α, β, d_c and C_{ste}. The first three are considered to be adjustable parameters of the model when fitting it to the measured profile. The last one is used for renormalization of the matrix **W** to the experimentally measured line widths.

The expression (6) is used to calculate part of the matrix **W** below diagonal, i.e. the elements W_{lk} with $l > k$, and these elements are proportional to the parameter C_{ste} which allow scaling them. Next, the experimentally measured broadening coefficients γ_k are substituted into the diagonal elements W_{kk}. Then De Niro renormalization is performed following [23] together with the calculation of

W_{lk} with $k > l$ using the sum rule (4). By this operation, scale parameter C_{ste} is excluded from the model and is not used further in the fit procedure.

4. Dissimilarity between the MPM and ECS approaches

The expression (6) allows calculation of the whole relaxation matrix **W**, regardless of its internal structure and branch interaction specifics. As it was mentioned before, **W** matrix, calculated within the MPM formalism is considered to be block-diagonal [21]:

$$\mathbf{W} = \begin{pmatrix} \mathbf{R} & 0 & 0 & 0 & 0 & 0 \\ 0 & \mathbf{R} & 0 & 0 & 0 & 0 \\ 0 & 0 & \mathbf{R} & 0 & 0 & 0 \\ 0 & 0 & 0 & \mathbf{R} & 0 & 0 \\ 0 & 0 & 0 & 0 & \mathbf{R} & 0 \\ 0 & 0 & 0 & 0 & 0 & \mathbf{R} \end{pmatrix},$$

where **R** is the submatrix of **W** responsible for intra-branch mixing supposed to be the same for each branch, while inter-branch ones are neglected and set to zero. To construct **W** matrix, one should take into account in each branch first n most intense transitions, whose contribution to absorption is most significant. Then, within the MPM approach, **W** matrix has size $6n \times 6n$, or 6×6 submatrices of size $n \times n$ (only six of them are non-zero and denoted as **R**, the other submatrices are filled with zeros). It includes n transitions in both $N+$ and $N-$ branches at positive and negative frequencies, and $2n$ non-resonant transitions, namely 0^+ and 0^- branches (while 0^0 lines are neglected).

Within the ECS formalism, we consider n strongest transitions of seven branches: n transitions in $N+$ and $N-$ branches at positive and negative frequencies, and n non-resonant transitions in 0^0, 0^+ and 0^- branches, consequently, the ECS matrix size is $7n \times 7n$ and has no constraints on the structure, i.e. non-diagonal blocks are not set to zero and diagonal blocks are not considered to be identical.

Moreover, within the MPM approach, coupling of the positive frequency lines with zero- and negative frequency ones is taken into account approximately through introduction of adjusted bias parameters (one can find more details in [21]). In the ECS model, all types of coupling are automatically generated from the definition of the matrix **W**.

Having calculated the matrix, one can use direct numerical inversion to calculate the absorption value according to the expression (1) or calculate first- and second-order mixing parameters and use the expression (3) derived from the perturbative approach. The discrepancy between the profiles calculated directly and in terms of the first- and second-order approximation derived from the same experimental profile record is shown in Fig. 1 together with the band profile calculated without collisional coupling taken into account as a sum of Van Vleck-Weisskopf profiles, i.e. the expression (3) with zero first- and second-order mixing coefficients. One can easily notice that, under these conditions, the contribution of the mixing effect is about 10% of the band

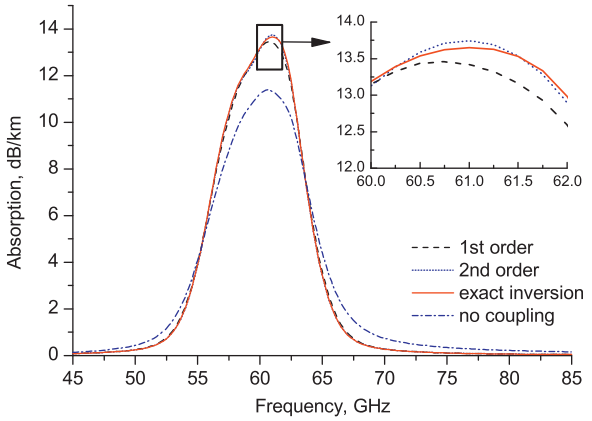

Fig. 1. Discrepancy between direct inversion in the expression (1) and calculation within the perturbation approach according to expression (3). The solid curve shows the oxygen band absorption profile calculated directly, dashed line shows one calculated using first-order approximation in pressure, the dotted line shows the profile calculated using first- and second-order approximation in pressure, the dashed dotted line shows the absorption band profile with neglected collisional coupling (i.e. the sum of Van Vleck-Weisskopf profiles). The first three profiles are calculated for the air at 300 K temperature and 750 Torr pressure and correspond to the optimization of the models to the same experimentally measured profile.

magnitude (separate contributions of the line mixing of the first and second order in terms of the observed profile minus a model fitted to the observed profile are shown in Fig. 12 of [4]). It is noticeable that near the band center the first-order profile underestimates the absorption value, while the second-order slightly overestimates it. This means that using different models for determining concentration one can get different values. In the following section oxygen concentration values obtained using the first-order MPM are compared with the ones obtained from the fit of the ECS model with direct numerical inversion to the measured band profile.

5. Determination of the ECS parameters

As was mentioned before, the relaxation matrix **W** can be defined by setting values of three adjustable parameters: α, β and d_c. The central frequencies and broadening coefficients (which are also used to exclude parameter C_{ste} in the expression (7), see Section 3) of the considered lines were earlier measured [4] at low pressure when line mixing is negligibly small. Line intensities are taken from the HITRAN database [25], and, as a result, the profile of the 60-GHz absorption band also depends on the three mentioned parameters.

It should be mentioned that there was small uncertainty of the oxygen concentration in the experimental data to which the model profile should be fit. In [12], the "first-order" MPM model profile was used to assess oxygen concentration for the band profile records. At the first step of the present work these values of the concentration were used as constant parameters. At the second step, the concentration was considered as an additional adjustable parameter because a more accurate

model should give smaller uncertainty of the determining concentration.

The parameter values corresponding to the best coincidence between model and experiment were found as the ones giving the lowest mean square residual between the measured and the calculated absorption. Application of the coordinate descent method has shown the existence of minimal mean square residual with regard to each adjustable parameter. From this fact we conclude that there should be a set of the mentioned four parameters values providing required minimal residual. This set of parameters gives relaxation matrix values for calculation of a model profile corresponding to the considered experimental record. The Levenberg–Marquardt algorithm was chosen for searching parameters giving minimal mean square residual for each experimental record. Parameters adjustment with the use of this algorithm was made twice: for four parameters, including oxygen concentration, and for three parameters with fixed concentration values taken from the previous work [12].

The initial concentration values determined by adjusting oxygen concentration in the first-order MPM to make the modeled band intensity correspond to the measured one are shown by diamonds in Fig. 2 together with the final concentration values obtained from the fit of the ECS model to the same experimental data set shown by circles. Values of the concentration obtained by the two models agree reasonably well with each other and therefore the procedure can be considered as a fine adjustment of the model. Despite the small value of the difference between two sets of concentration values, analysis of the values of α, β and d_c obtained from the fit shows that taking oxygen concentration into account makes a noticeable change in other parameter values and leads to a better agreement of the ECS model with the experiment.

Figs. 3–5 show the obtained values of α, β and d_c parameters at various temperatures for both ways of adjustment. Regular dependence of each parameter on temperature (or regular constant value) should be used for the absorption band model to be valid at any temperature value within the studied temperature range. Parameter α shows weak linear dependence on temperature. To demonstrate that β and d_c are temperature

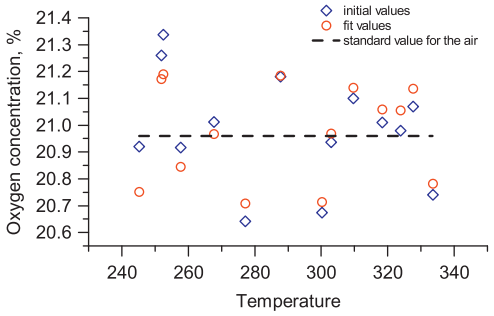

Fig. 2. Oxygen concentration in the air sample at various temperatures. The circles show fit values obtained with oxygen concentration taken as an additional variable parameter, diamonds – initial values obtained by adjustment of oxygen concentration in first-order MPM until modeled band intensity corresponds to the measured one.

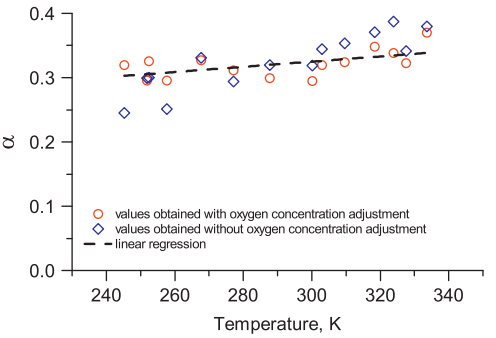

Fig. 3. α parameter versus temperature. The circles show fit values obtained with oxygen concentration taken as an additional adjustable parameter, diamonds – fit values obtained without it. The dashed line shows linear regression of the fit values shown by circles versus temperature.

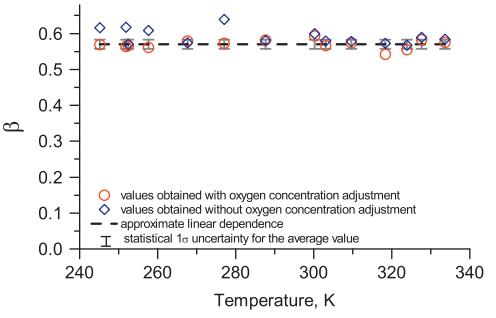

Fig. 4. β parameter versus temperature. The circles show fit values obtained with oxygen concentration taken as an additional adjustable parameter, diamonds – fit values obtained without it. The dashed line shows linear regression of the fit values shown by circles versus temperature, error bars show statistical uncertainty of the averaged parameter value.

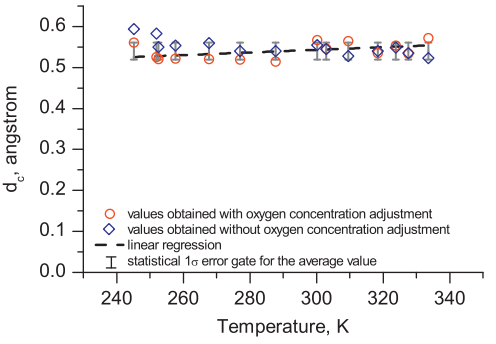

Fig. 5. d_c parameter versus temperature. The circles show fit values obtained with oxygen concentration taken as an additional adjustable parameter, diamonds – fit values obtained without it. The dashed line shows linear regression of the fit values shown by circles versus temperature, error bars show statistical uncertainty of the averaged parameter value.

independent, linear regression of β and d_c versus temperature is presented in Figs. 4 and 5 by dashed line together with the corresponding parameter mean value and its statistical uncertainty range (shown by error bars). It is clearly seen that within this range both lines for β and d_c might be considered as having zero slope. Also, it is

noticeable that values obtained with fixed oxygen concentration have greater scatter, which also points to the necessity of considering oxygen concentration as an adjustable parameter. Independence of d_c on temperature was expected according to the following general considerations. This parameter corresponds to the specific range of the dominant intermolecular potential, i.e. being a "micro-parameter", it should not depend on temperature, which is "macro-parameter" defined by mean kinetic energy of the molecular translational motion.

In the final model, following parameter values are used for calculating the relaxation matrix: $\alpha(T) = 0.086 + 8.154 \cdot 10^{-4} T$, $\beta = 0.5805$, $d_c = 0.545$ Å.

6. Difference between experimental and calculated profiles

It is interesting to compare the residuals given by the second-order MPM extension [12] and the ECS model. Fig. 6 shows residuals for six selected temperature values. It is worth noting that both approaches provide great accuracy in reproducing the experimental data and the difference between two models is noticeable only when analyzing magnified measurement-minus-calculation residuals. The dotted curves in Fig. 6 are for the residual given by the second-order MPM having parameters obtained from the same experimental data set and smoothed over the covered temperature range (see [12] for details), the solid curves are for the residual given by the ECS model with parameters given above. One can see that the difference between two models at temperatures above 300 K is small: the difference between standard deviations of two residuals is small, as well as the difference between maximal-minus-minimal values of the mentioned residuals. At lower temperatures ECS calculated absorption is noticeably closer to the measured value than the MPM one. This can be explained by the fact that a decrease of the temperature leads to an increase of line widths, which consequently increases line profiles overlapping. This leads to a greater impact of collisional coupling, including interbranch coupling which is neglected within the MPM approach. Irregular outlying points in the ECS residuals are most likely related to the measurement noise which is more prominent near the band center as discussed in [12].

7. ECS and MPM relaxation matrices

7.1. MPM assumptions verification

Fig. 7 shows matrix elements W_{lk} at $k = 9+$ and $k = 13+$ for both ECS and MPM calculated matrix. As was mentioned earlier, inter-branch coupling is neglected in the MPM matrix which results at zero values for negative N, but the ECS matrix elements show that the matrix elements responsible for inter-branch coupling are quite large and should be taken into account for precise calculations.

Another MPM assumption was equivalence of the submatrices of **W** responsible for intra-branch coupling of different branches. Panel (a) of Fig. 8 shows as a typical example that the elements of ECS matrix **W** responsible for coupling line $N = 13+$ with other positive frequency lines almost coincide with those mirrored with respect to zero elements responsible for coupling line $N = 13-$ with other positive frequency lines. Panel (b) of Fig. 8 shows that the difference between the corresponding values of **W** elements are approximately two orders of magnitude lower than the values of the elements, which points to the fact that the mentioned assumption used in the MPM approach is reasonable.

7.2. Validation of the first- and second-order perturbation approach

Similarly to the MPM relaxation matrix, the ECS matrix allows calculating first-order mixing parameters to be used in a model profile constructed using the perturbation theory approach. These parameters derived from both matrices are shown in Fig. 9. One can notice that the MPM parameters look like "smoothed" ECS ones. The oscillatory behavior of the ECS y-s is a result of the "resonance effects" arising when pairs of weakly coupled but having close central frequency lines neglected in MPM are taken into account. For instance, one can consider weakly coupled ($W_{13+,3-} = 0.023$ MHz/Torr) $13+$ and $3-$ lines spaced apart by 48.9 MHz. The contribution of coupling between these two lines to the magnitude of y_{13+} will be significant compared to the contribution of the coupling between line $13+$ and other lines. This leads to a noticeable difference of the mixing parameter y_{13+} from the parameters with close N values. The contribution of coupling between $13+$ and $3-$ lines is:

$$2\frac{d_{3-}}{d_{13+}}\frac{W_{3-,13+}}{f_{13+}-f_{3-}} = 351.3 \cdot 10^{-5}\ 1/\text{Torr} > 0$$

in y_{13+} and

$$2\frac{d_{13+}}{d_{3-}}\frac{W_{13+,3-}}{f_{3-}-f_{13+}} = -8.094 \cdot 10^{-5}\ 1/\text{Torr} < 0$$

in y_{3-}, which explains relative positions of the corresponding parameters with respect to the smoothed curve provided by MPM. One can compare the contribution of coupling between the lines $13+$ and $3-$ with the contribution of coupling of the line $13+$ with two nearest $N+$ lines, $11+$ and $15+$ (one can see in Fig. 7 that matrix elements W_{lk} for coupling between the line $13+$ with the two mentioned lines have the highest absolute value) and with the line $5-$. The corresponding calculated values are -133.5, 79.46 and -7.210 in units of 10^{-5}/Torr.[2] From these calculations one can conclude that, due to small central frequency difference, the coupling between the $13+$ and $3-$ lines belonging to different branches is as strong as the coupling between the line $13+$ and the nearest lines of the same branch. At the same time, the contribution of $13+$ line coupling with other lines in $N-$ is approximately two orders of magnitude lower. In the

[2] To calculate all the mentioned values we used the ECS matrix. Using the MPM matrix for the first two ones gives -165.0 and 10.44 10^{-5}/Torr, respectively, which is close to the values calculated using the ECS matrix.

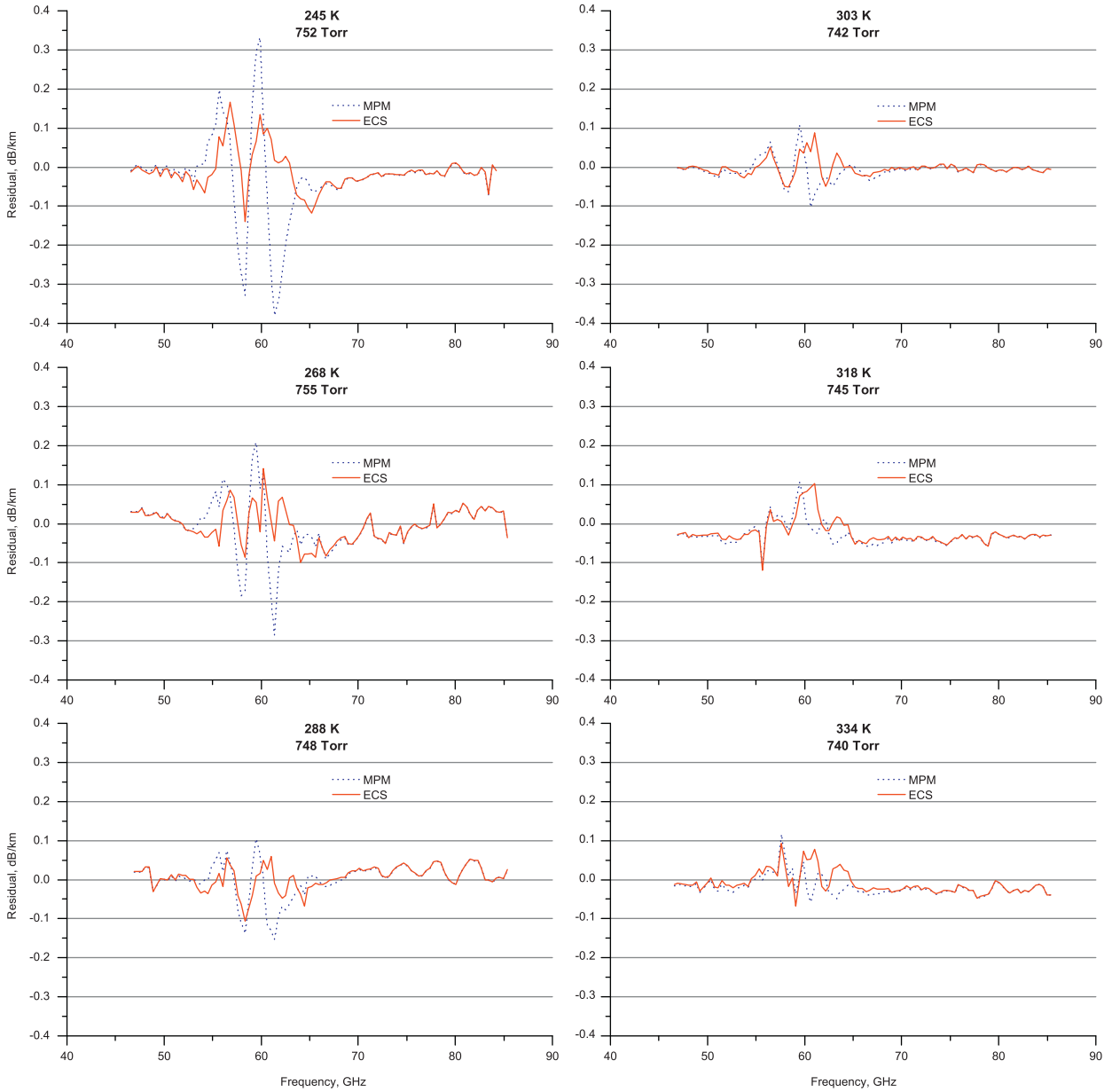

Fig. 6. Difference between measured band profile and various calculated profiles at various temperatures. The dotted line is for the MPM calculated profile from [12], the solid line is for the ECS profile calculated with smoothed parameters (see Section 5).

MPM, by virtue of zero $W_{13+,3-}$, there are no contributions that would lead to a smooth behavior of y parameters against quantum number.

Line $N=1-$ deserves a special comment. It is located at the frequency of 118.75 GHz and is relatively isolated from the other lines. The first-order mixing parameter of this line has been measured directly in [8] giving y_{1-} value of $-5.5(3)$ 10^{-5}/Torr at 300 K, and the value derived from the ECS matrix **W** is -3.8 10^{-5}/Torr, which may be considered as a rather good coincidence, as y parameter for this line is one of the weakest values resulting from a great amount of compensating effects. Moreover, one may recall that, within this study, we have neglected difference between O_2 and N_2 as a collisional partner which is not completely true because values of y_{1-} are different when measured in dry air and pure O_2[8].

The second-order parameters derived from the ECS matrix also show great difference from MPM ones (see Figs. 10 and 11) for the majority of the lines. The expressions for g and $\delta\nu$ include products of two relaxation matrix elements and two central frequency differences (see Eqs. (15) and (16) in [11]), which leads to the greater influence of the "resonance effects" discussed above.

7.3. Possibility of simplified calculations

It should be emphasized that, under the aforementioned assumptions, ECS calculations are "exact", i.e.

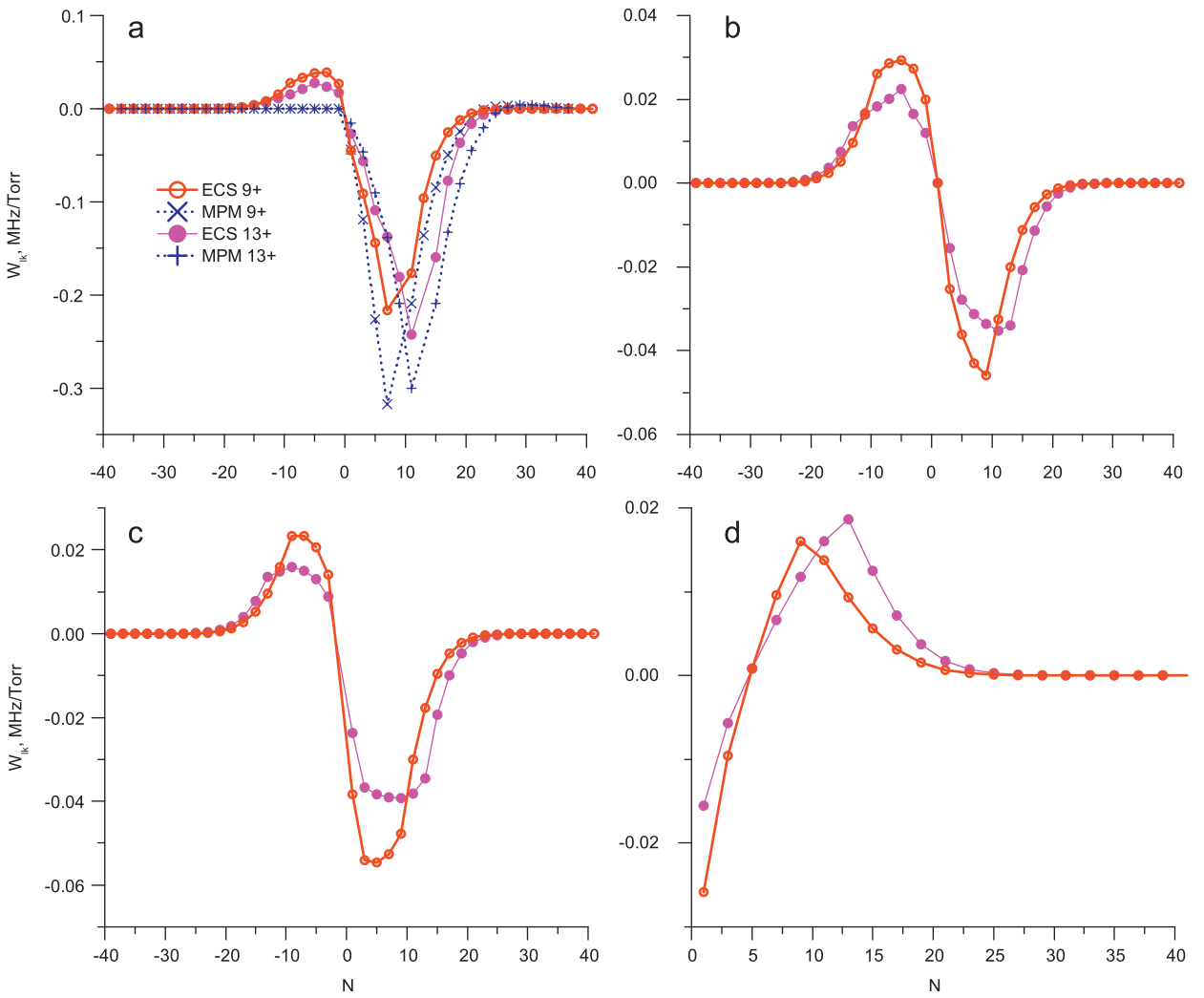

Fig. 7. Matrix elements for coupling of the line $N=9+$ (hollow points) and $N=13+$ (filled points) with other fine structure lines: (a) with the lines of $N\pm$ branches at positive frequencies, (b) $N\pm$ branches at negative frequencies, (c) $0_N^{\pm}$ lines, (d) 0^0 lines. Circles and solid lines show ECS matrix elements, crosses and dashed lines show MPM ones.

obtained from a direct inversion of the $(\mathbf{I}f-\mathbf{f}_0-iP\mathbf{W})$ matrix. However, if one considers only narrow spectral region from 45 to 75 GHz, some reasonable additional assumptions can possibly lead to a simpler formalism based on the fact that at atmospheric pressure oxygen absorption profile appears as three isolated features near $+60$ GHz, -60 GHz and 0 GHz. It allows neglecting coupling between positive, negative and non-resonant blocks (in [11] they are denoted as Ω^+, Ω^- and Ω^0), which leads to a block-diagonal matrix **W**. Also, the far wing of the non-resonant contribution to absorption near 60 GHz can be written as

$$\sum_{k,l\in\Omega^0}\rho_k d_k d_l \frac{W_{lk}}{(f-f_l)(f-f_k)}\cdot\left(\sum_{k\in\Omega^0}\rho_k d_k^2\right)\frac{\gamma_{eff}}{(f-f_\Omega^0)^2},$$

where γ_{eff} is equivalent half-width of the Lorentzian profile describing the non-resonant part of oxygen spectrum [2] given by the following expression:

$$\gamma_{eff}=\left(\sum_{k\in\Omega^0}\rho_k d_k^2\right)^{-1}\times\sum_{k,l\in\Omega^0}\rho_k d_k d_l W_{lk}=0.778\ \text{MHz/Torr}.$$

The independently determined value 0.746 MHz/Torr used in the MPM is in good agreement with the ECS prediction given above. In the submillimeter-wave range, by virtue of $f_\Omega^0=0$ the contribution of the Ω^0 branch multiplied by $f\cdot(1-e^{\beta hf})\approx\beta hf^2$ is constant and very small compared to the resonance absorption. One can find that MPM also uses this approach to the non-resonant absorption in molecular oxygen, which was described by Van Vleck [2].

A similar consideration can be made for the contribution of the Ω^- branch, so one may consider the only branch Ω^+ as giving the most significant contribution to absorption value. This contribution may be calculated either by direct inversion or by the perturbation theory

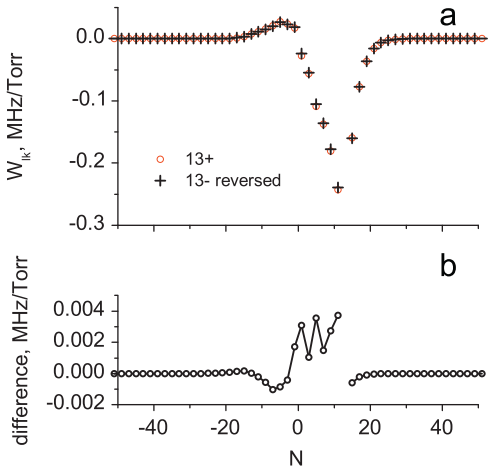

Fig. 8. Matrix elements for coupling of the lines $N=13+$ and $N=13-$ with other positive frequency lines: (a) matrix elements for $N=13+$ together with the ones reversed with respect to $N=0$ elements for $N=13-$; (b) difference between values shown in the upper part of the figure.

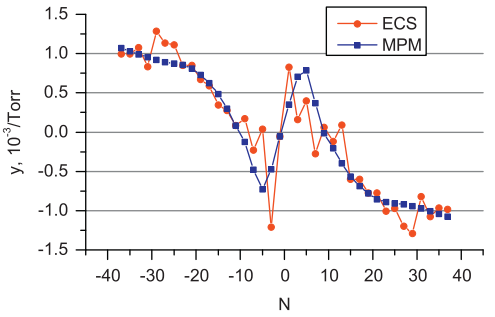

Fig. 9. First-order mixing coefficients derived from the MPM (squares) and ECS (circles) relaxation matrices.

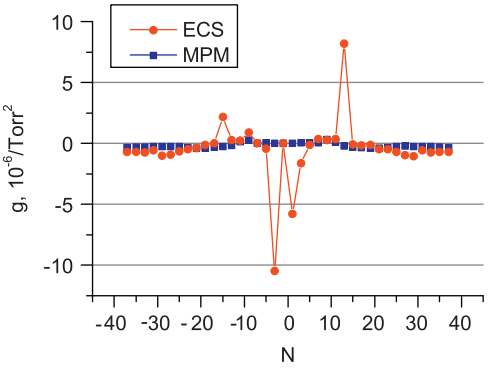

Fig. 10. Second-order mixing parameters g derived from MPM (squares) and ECS (circles) relaxation matrices.

approach. Results of the both considering only Ω^+ part of the ECS matrix are shown in Fig. 12: the second-order "perturbative" absorption model (dashed line) is close enough to the "exact" model (solid line), however, some large discrepancies between two models are seen in a small spectral region around 62.5 GHz, which corresponds

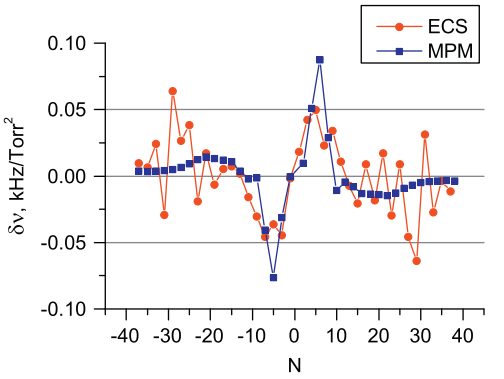

Fig. 11. Second-order mixing parameters $\delta\nu$ derived from MPM (squares) and ECS (circles) relaxation matrices.

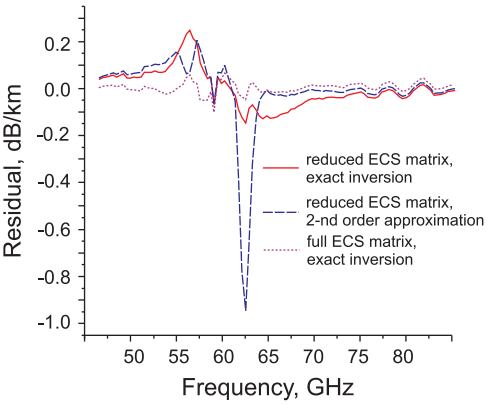

Fig. 12. Residuals between measured and modeled absorption using various simplified approaches at 300 K and 750 Torr. The solid line shows residual calculated using part of the ECS matrix for positive-frequencies lines and exact inversion, the dashed line shows residual obtained using the same part of ECS matrix and second-order approximation, the dotted line shows residual for full ECS matrix and exact inversion.

exactly to the $N=13+$ and $N=3-$ oxygen lines. It was demonstrated above that these lines are too close to permit a convenient perturbative treatment with the ECS matrix.[3] For comparison, the residual obtained when using a full ECS matrix and exact inversion is also shown in Fig. 12. We can conclude that, on the one hand, it is possible to neglect coupling of the positive frequency branches with non-resonant and negative frequency branches. On the other hand, the ECS approach provides physically justified model taking into account coupling of all fine structure transitions branches. The advantage of this approach is most pronounced at low temperatures, as it is demonstrated by Fig. 6. Neglecting relatively small coupling of the positive frequency branches with other branches results in noticeable difference between calculated and measured absorption values. Within the MPM approach, the mentioned neglected coupling with

[3] Nevertheless, as the coupling between $N+$ and $N-$ lines is not considered in MPM, we can assess that the differences between the inversion and the second order perturbation theory treatment should be smaller.

non-resonant and negative frequency branches, as well as neglected coupling between positive frequency $N+$ and $N-$ branches is partially compensated by a greater magnitude of **W** elements responsible for intra-branch coupling.

8. Conclusions

As compared to the MPM approach, even extended to the second order [12], the ECS approach is physically preferable for calculation of molecular oxygen absorption profile under atmospheric pressure in the case of appreciable collisional coupling effect and gives a model absorption profile closer to the measured one. Better agreement between the measured values of absorption and the ones calculated using the ECS approach is observed at temperatures below 300 K. This is explained by more rigorous allowance for collisional coupling whose influence is stronger at low temperatures. At the same time, at temperatures above 300 K both the discussed models give close results that agree with the measurements.

The relaxation matrix calculated with the ECS methods can be used to derive absorption profile using direct inversion or the second-order perturbation theory. It was shown that, having calculated the ECS relaxation matrix, one can neglect the impact of the non-resonant and negative-frequency branches and use the approximated expressions to calculate their contribution, which will result in residuals of approximately two times greater magnitude than those obtained using the full ECS matrix. The advantage of the proposed simplified method is the fact that direct inversion with a limited number of lines is faster than inversion of the full matrix.

Further improvement of modeling accuracy is possible by obtaining further experimental data. First, oxygen absorption profiles can be measured in pure oxygen, and, also, in the mixture of molecular oxygen and nitrogen with low concentration of oxygen, which will give information on separate relaxation matrices for oxygen and nitrogen, respectively. Another possibility of modeling accuracy improvement is measurement of temperature behavior of the fine structure lines broadening coefficients depending upon quantum number N.

Acknowledgments

This work was partially supported by RFBR. The authors are grateful to Philip W. Rosenkranz for the information on the theory for MPM construction.

References

[1] Rosenkranz PW. Shape of the 5 mm oxygen band in the atmosphere. IEEE Trans Antennas Propag 1975;23(4):498–506.
[2] Van Vleck JH. Magnetic dipole radiation and atmospheric absorption bands of oxygen. Astrophys J 1934;80:161–70.
[3] Liebe HJ. MPM – an atmospheric millimeter-wave propagation model. Int J Infrared Mill Waves 1989;10:631–50.
[4] Tretyakov MYu, Koshelev MA, Dorovskikh VV, Makarov DS, Rosenkranz PW. 60-GHz oxygen band: precise broadening and central frequencies of fine structure lines, absolute absorption profile at atmospheric pressure, revision of mixing coefficients. J Mol Spectrosc 2005;231:1–14.
[5] Sñhulze AE, Tolbert CW. Shape, intensity and pressure broadening of the 2.53-millimetre wave-length oxygen absorption line. Nature 1963;200:747–50.
[6] Tretyakov MYu, Golubiatnikov GYu, Parshin VV, Koshelev MA, Myasnikova SE, Krupnov AF, et al. Experimental study of the line mixing coefficient for 118.75 GHz oxygen line. J Mol Spectrosc 2004;223:31–8.
[7] Tretyakov MYu, Koshelev MA, Koval IA, Parshin VV, Kukin LM, Fedoseev LI, et al. Temperature dependence of pressure broadening of the $n=1$-fine structure oxygen line at 118.75 GHz. J Mol Spectrosc 2007;241(1):109–11.
[8] Makarov DS, Koval IA, Koshelev MA, Parshin VV, Tretyakov MYu. Collisional parameters of the 118-GHz oxygen line: temperature dependence. J Mol Spectrosc 2008;252:242–3.
[9] Baranger M. Problem of overlapping lines in the theory of pressure broadening. Phys Rev 1958;111(2):494–504.
[10] Fano U. Pressure broadening as a prototype of relaxation. Phys Rev 1963;131(1):259–68.
[11] Smith EW. Absorption and dispersion in the O_2 microwave spectrum at atmospheric pressures. J Chem Phys 1981;74(12):6658–73.
[12] Makarov DS, Tretyakov MYu, Rosenkranz PW. 60-GHz oxygen band: precise experimental profiles and extended absorption modeling in a wide temperature range. J Quant Spectrosc Radiat Transfer 2011;112(9):1420–8.
[13] Boukabara S-A, Clough SA, Moncet J-L, Krupnov AF, Tretyakov MYu, Parshin VV. Uncertainties in the temperature dependence of the line-coupling parameters of the microwave oxygen band: impact study. IEEE Trans Geosci Remote Sensing 2005;43(5):1009–114.
[14] Boukabara SA, Clough SA, Moncet J-L, Krupnov AF, Tretyakov MYu, Parshin VV. Reply to the Comment on "Uncertainties in the temperature dependence of the line-coupling parameters of the microwave oxygen band: impact study". IEEE Trans Geosci Remote Sensing 2005;43(5):2161–2.
[15] Tretyakov MYu, Krupnov AF, Koshelev MA, Makarov DS, Serov EA, Parshin VV. Resonator spectrometer for precise broadband investigations of atmospheric absorption in discrete lines and water vapor related continuum in millimeter wave range. Rev Sci Instrum 2009;80:093106-1–10.
[16] Gordon RG. Semiclassical theory of spectra and relaxation in molecular gases. J Chem Phys 1966;45(5):1649–55.
[17] Lam KS. Application of pressure broadening theory to the calculation of atmospheric oxygen and water vapor microwave absorption. J Quant Spectrosc Radiat Transfer 1977;17:351–83.
[18] Tran H, Boulet C, Hartmann J-M. Line mixing and collision-induced absorption by oxygen in the A-band: laboratory measurements, model, and tools for atmospheric spectra computations. J Geophys Res 2006;111:D15210.
[19] Ben-Reuven A. Transition from resonant to nonresonant line shape in microwave absorption. Phys Rev Lett 1965;14(10):349–51.
[20] Hartmann J-M, Boulet C, Robert D. Collisional effects on molecular spectra. Elsevier; 2008.
[21] Rosenkranz PW. Interference coefficients for overlapping oxygen lines in air. J Quant Spectrosc Radiat Transfer 1988;39:281–97.
[22] Corey GC, McCourt FR, Liu WK. Hyperfine effects on collisional line shape. I. A self-consistent set of equations. J Phys Chem 1984;88:2031.
[23] Niro F, Boulet C, Hartmann J-M. Spectra calculations in central and wing regions of CO_2 IR bands between 10 and 20 μm. I: model and laboratory measurements. J Quant Spectrosc Radiat Transfer 2004;88:483–98.
[24] DePristo AE, Augustin SD, Rabitz HR. Quantum number and energy scaling for nonreactive collisions. J Chem Phys 1979;71:850–65.
[25] Rothman LS, Gordon IE, Barbe A, Benner DC, Bernath PF, Birk M, et al. The HITRAN 2008 molecular spectroscopic database. J Quant Spectrosc Radiat Transfer 2009;110:533–72.